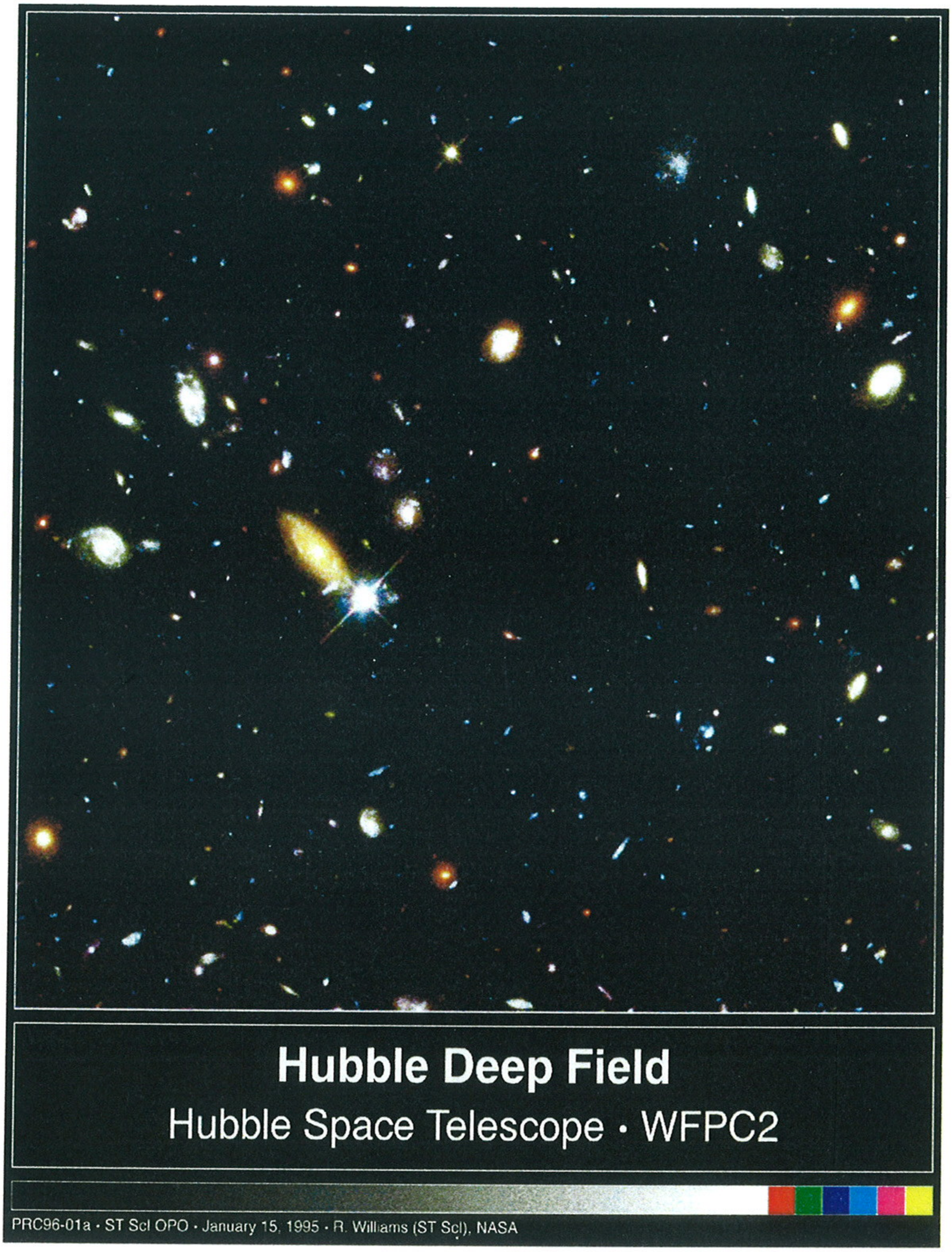
Hubble Deep Field
Hubble Space Telescope • WFPC2
PRC96-01a · ST ScI OPO · January 15, 1995 · R. Williams (ST ScI), NASA

Fig. 1,2

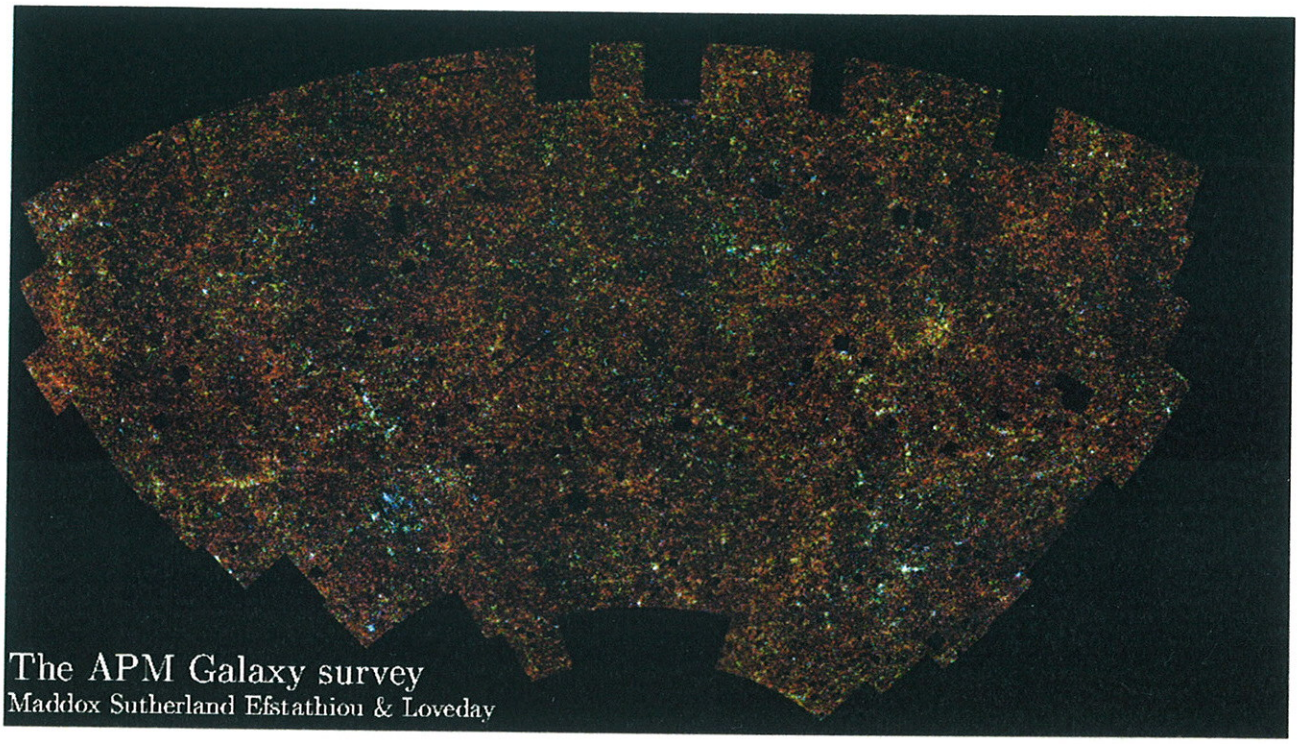
The APM Galaxy survey
Maddox Sutherland Efstathiou & Loveday

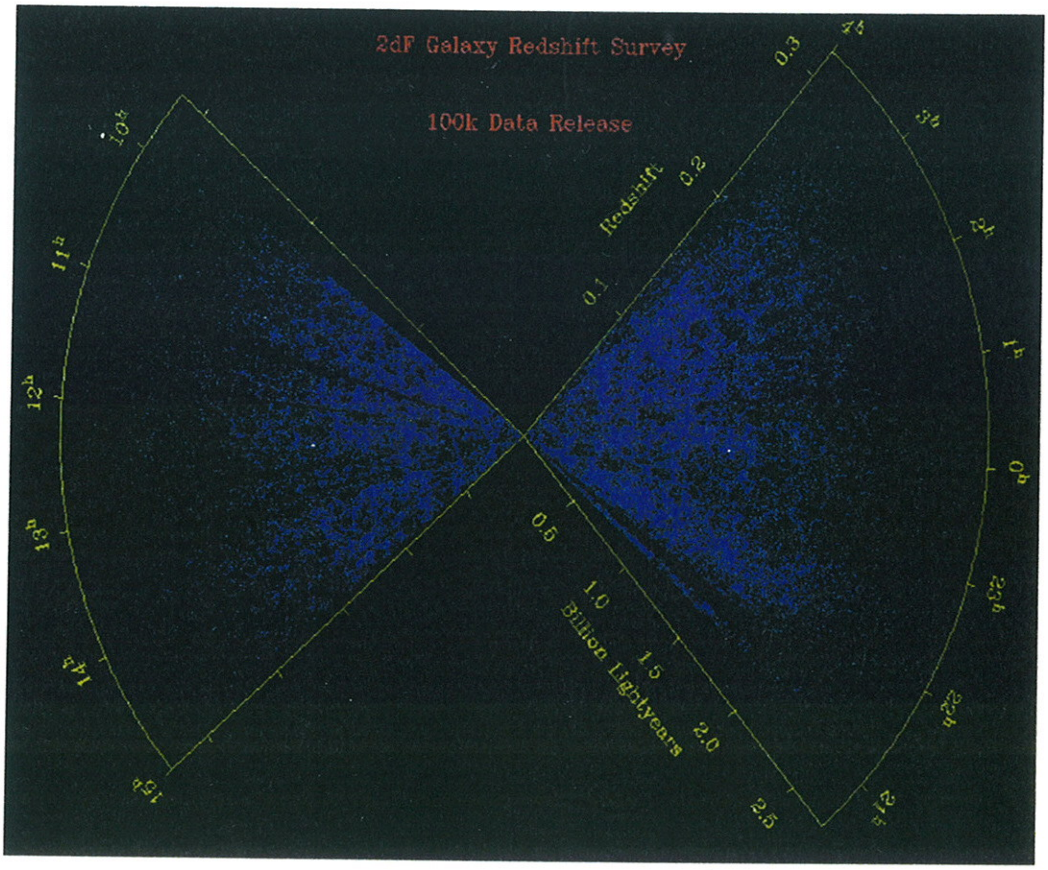
2dF Galaxy Redshift Survey
100k Data Release
Redshift
0.1
0.2
0.3
0.5
1.0
1.5
2.0
2.5
Billion Lightyears
10h
11h
12h
13h
14h
15h
4h
3h
2h
1h
0h
23h
22h
21h

Fig. 1.3

Lyman α
720 nm

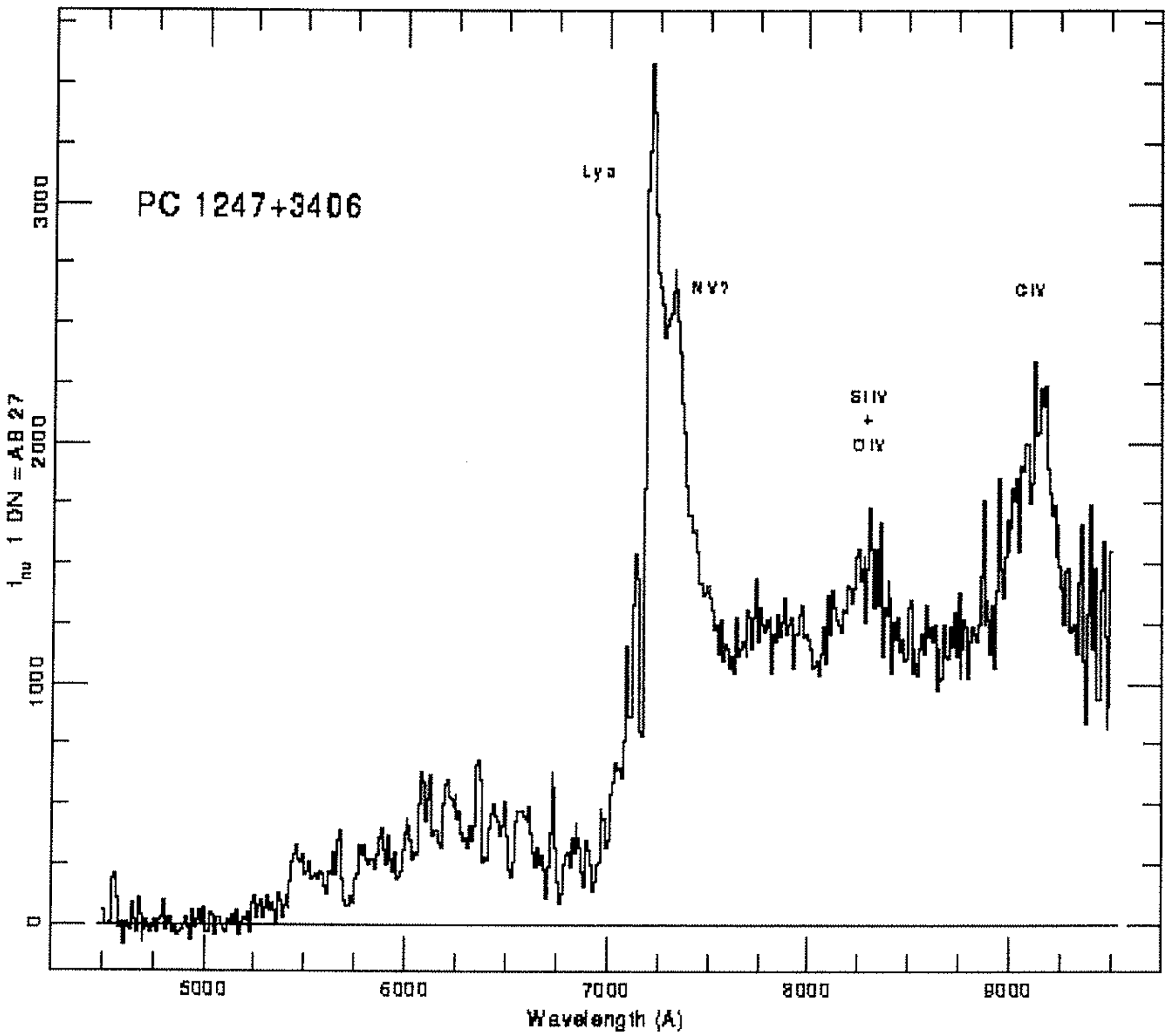

z = 4.897

Fig 1.4

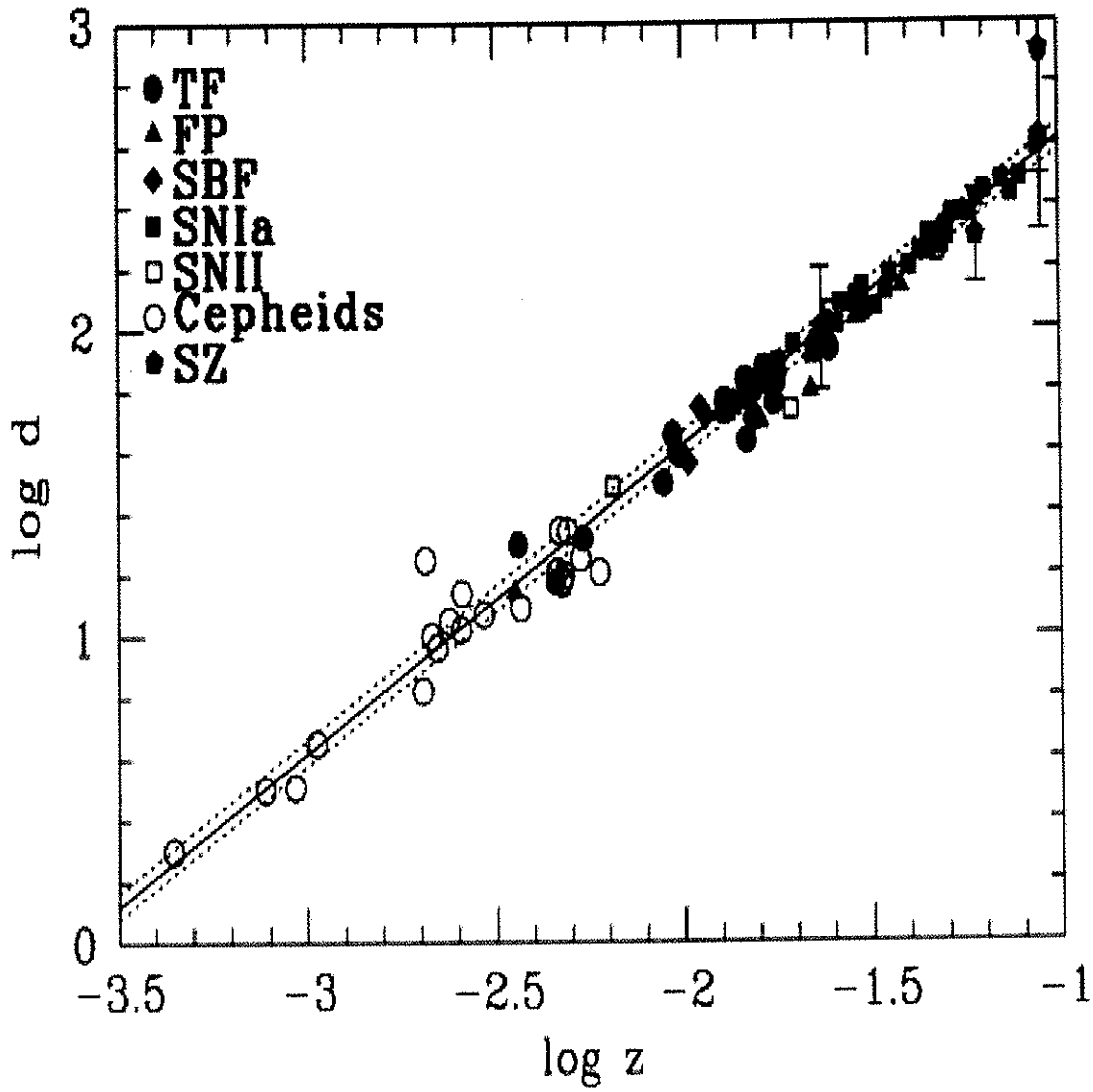

Fig 1.6

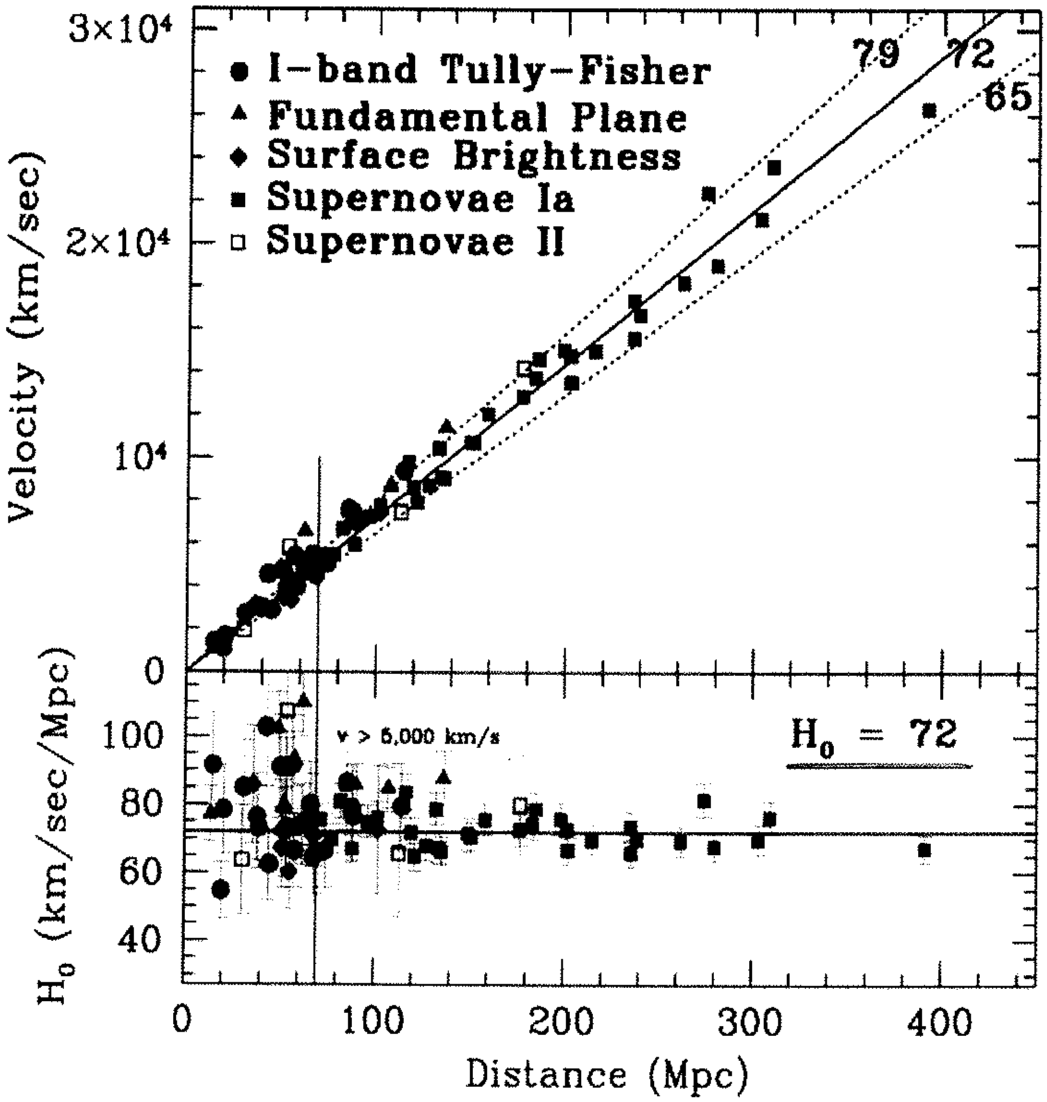
3×10⁴
2×10⁴
10⁴
0
Velocity (km/sec)
I-band Tully-Fisher
Fundamental Plane
Surface Brightness
Supernovae Ia
Supernovae II
79
72
65
100
80
60
40
H₀ (km/sec/Mpc)
v > 5,000 km/s
H₀ = 72
0
100
200
300
400
Distance (Mpc)

Fig. 1.7

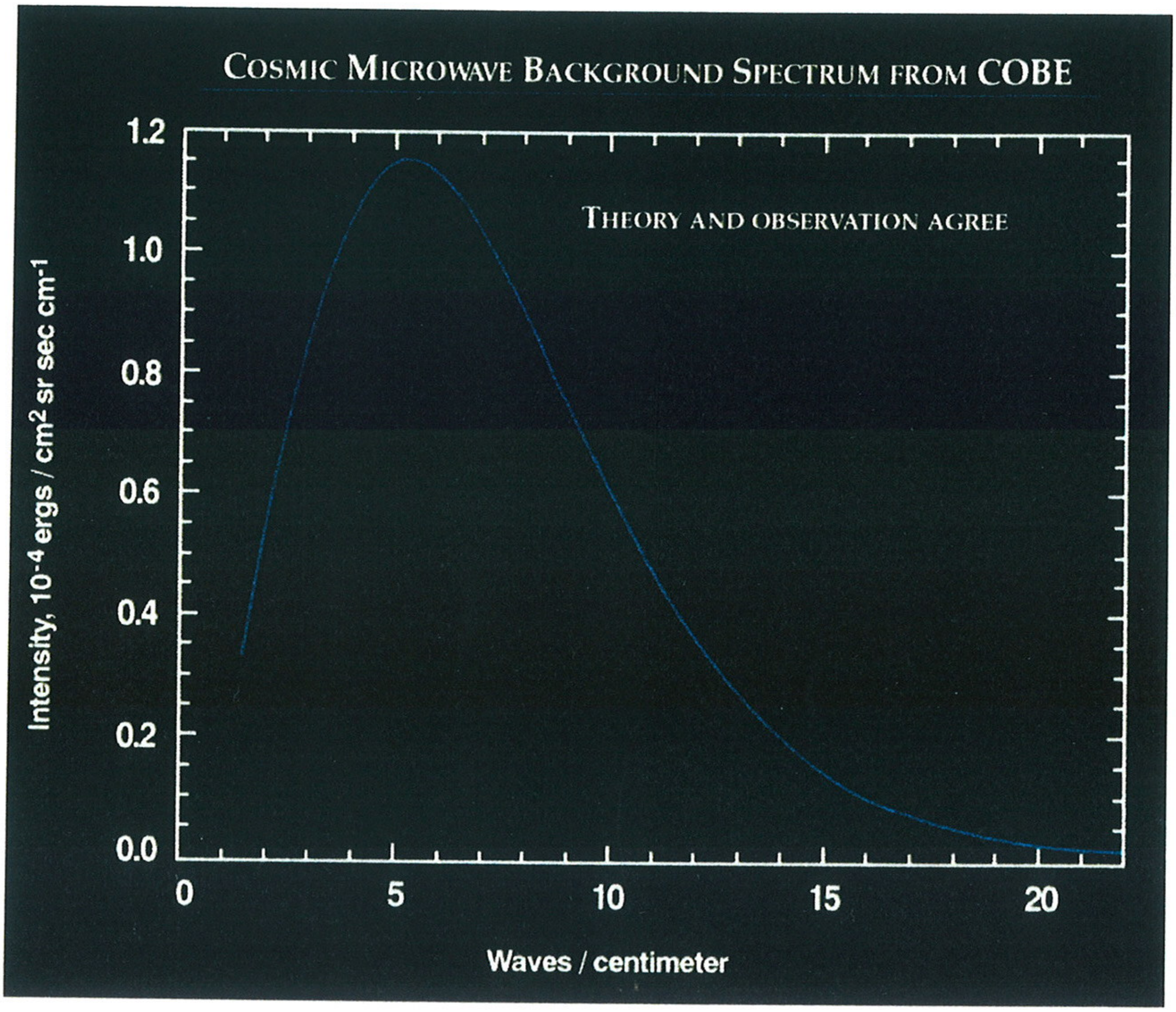

$T = 2.728 \pm 0.004$ K

Fig 1.8

courtesy COBE / NASA

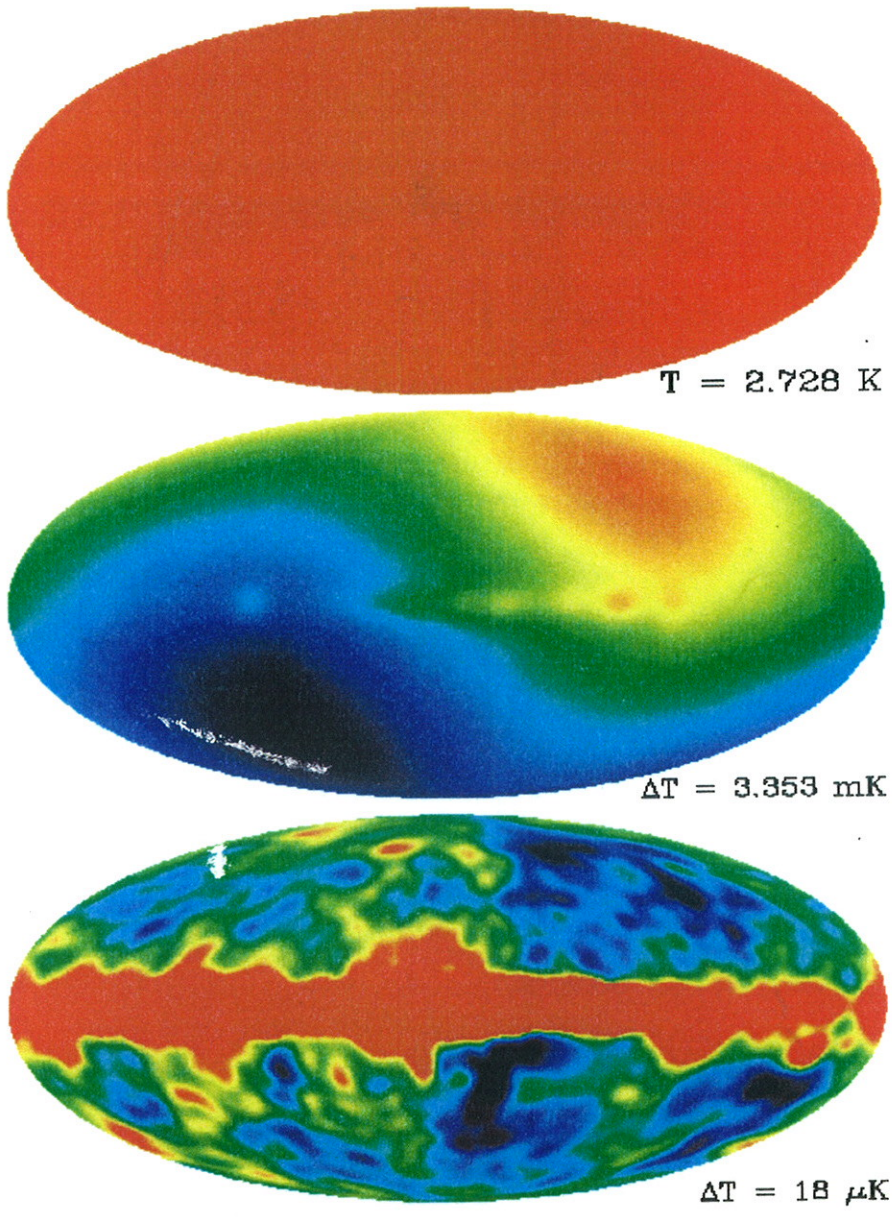

Fig 1.9.

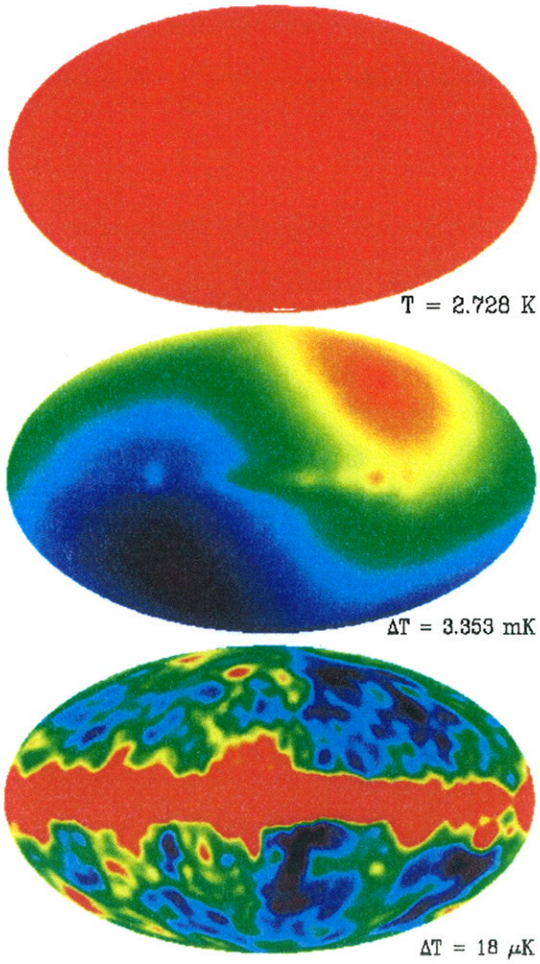

Fig. 1.9. The four year temperature maps of the microwave background from the COBE satellite. Darker (lighter) regions correspond to cooler (hotter) ares. These are all sky maps measured in galactic coordinates, where the plane of the galaxy runs along the horizontal and Sagittarius is in the centre. COBE measured the difference in temperature between two given directions separated by 10^o. The top map is what is observed to a sensitivity of one part in 10^4. The radiation is uniform at this level of accuaracy. The second shows that the radiation is warmer in one direction by about 0.007 K. This is interpreted as a Doppler effect due to the motion of our Galaxy relative to the rest of the universe at a speed of some $600 \mathrm{km\,s^{-1}}$. The bottom map shows what is left when this is subtracted out – the radiation is very nearly uniform to 1 part in 10^5, but small temperature differences are observed. (The band along the horizontal is due to emission from the galactic plane and should be ignored). The COBE datasets were developed by the NASA Goddard Space Flight Center under the guidance of the COBE Science Working Group and were provided by the NSSDC.

(also Fig 1.9)

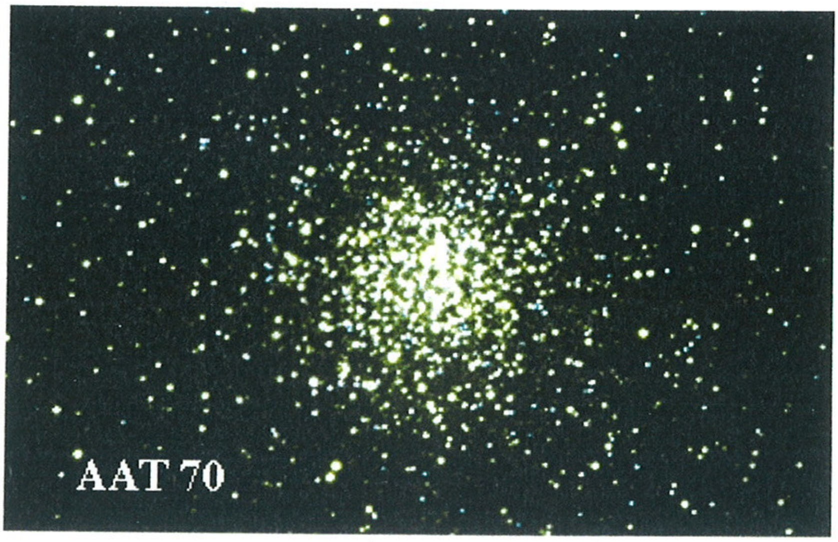

Globular clusters contain between 0.1-1 million stars that are gravitationally bound into a single structure some 100 light years across. They are generally spherically symmetric. Stars in a globular cluster have similar chemical compositions impying that they have similar ages. Globular clusters are some of the oldest systems in the universe. This is a picture of the globular cluster M5, first discovered in 1702. It is one of the oldest clusters with an age thought to be around 13 billion years.

Fig 5.5

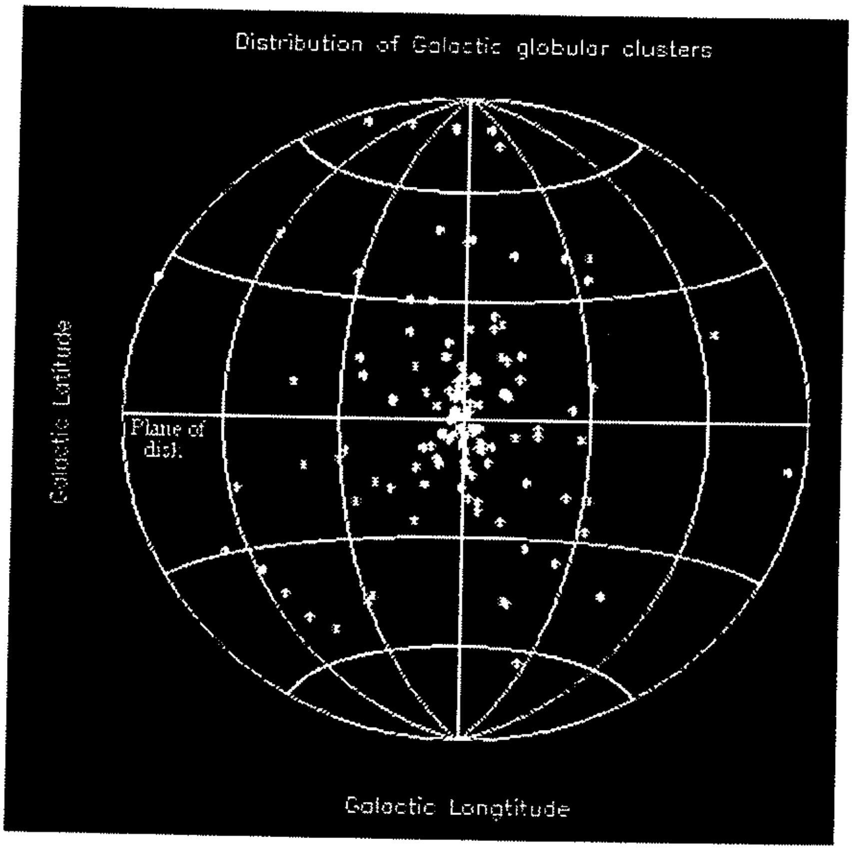

There are over 150 globular clusters in our Galaxy. This figure shows their distribution, plotted in galactocentric coordinates such that the centre of the plot corresponds to the centre of the galaxy and the plane of the galaxy runs along the central horizontal axis. Globular clusters are distributed in a spherical halo around the galactic centre. This indicates that they formed during the early phase of the Galaxy's history and before the galactic material had formed into a disc. Further evidence that globular clusters are old is deduced from their chemical composition. The abundances of heavier elements in globular clusters is significantly lower than in second generation stars such as the Sun, implying that they formed out of mainly primordial matter (rather than matter from supernovae remnants).

Fig 5.6

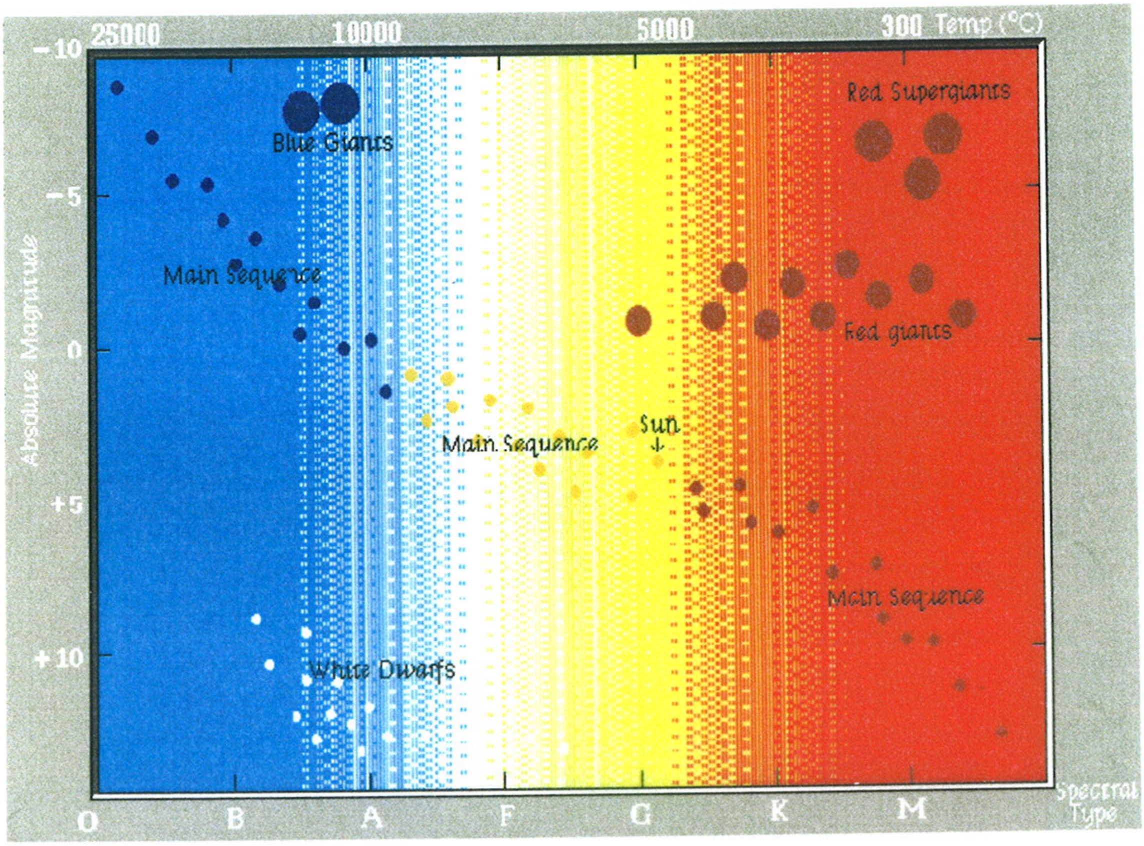

The age of a globular cluster is deduced from the Hertzsrung-Russel (HR) diagram that plots a star's luminosity with its temperature (cf. your stellar structure lectures). Both these quantities are determined by star's mass. Hence the position of a star on the HR diagram is determined by its mass. Most stars lie on the Main Sequence – a diagonal band running from the bottom–right to the top–left of the diagram. This is the phase where hydrogen in the stellar core is fused to helium. More massive stars are more luminous and evolve off the main sequence more rapidly than a low mass star.

Fig 5.7

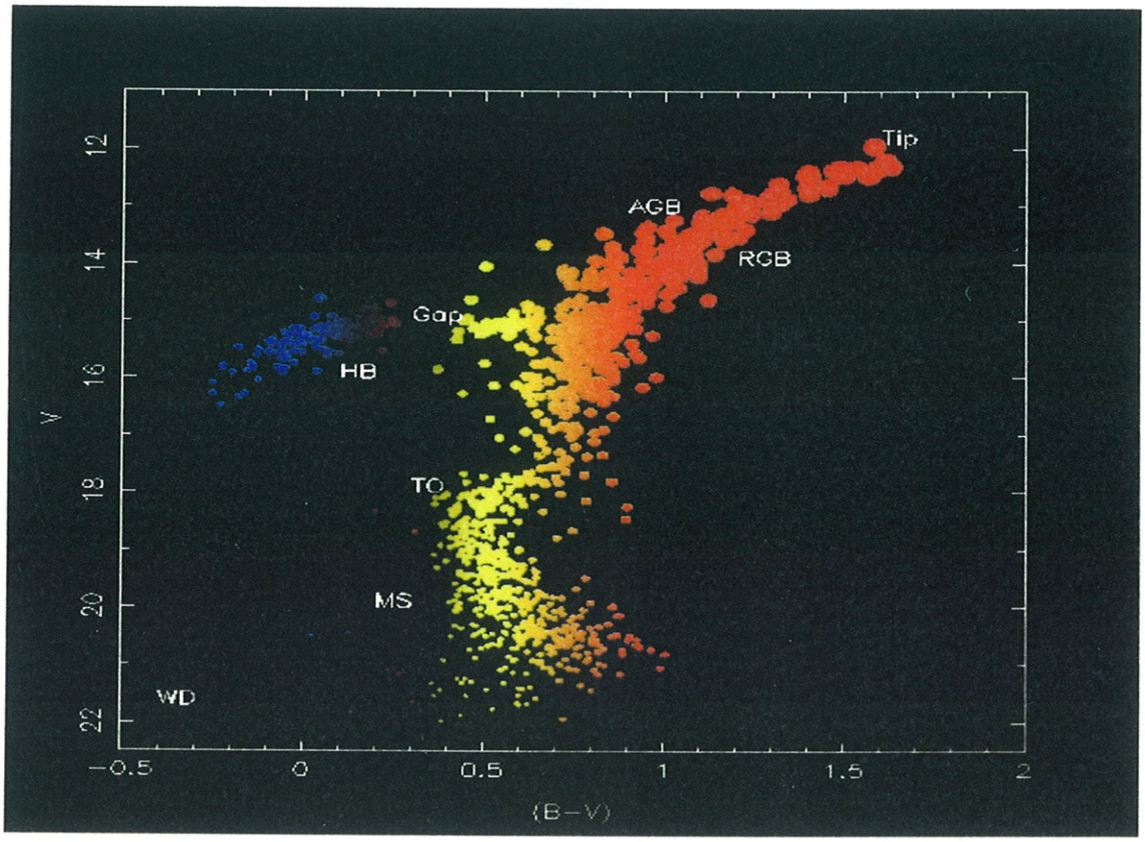

The HR diagram for the globular cluster M5. Stars of a given globular cluster have a similar history, in that they have a similar chemical composition. They therefore differ only in their masses. Consequently, the stars in a newlym formed globular cluster are distributed along the main sequence over a range of masses. As time proceeds, the more massive stars turn off the main sequence sooner than their low mass siblings. Thus, the older the globular cluster, the higher the number of stars that have turned off the main sequence. The turn–off point (TO) is their lower in the diagram, i.e., the main sequence band is shorter. The age of a globular cluster is then determined by the position of the turn–off point. A numerical estimate for the age is deduced by fitting a theoretical model for the evolution of the stars with the observed data.

Fig 5.8

The HR diagram for the globular cluster M5, as before, this time showing the theoretical curves for three stellar ages, corresponding to 10, 12 and 14 Gyr, respectively.

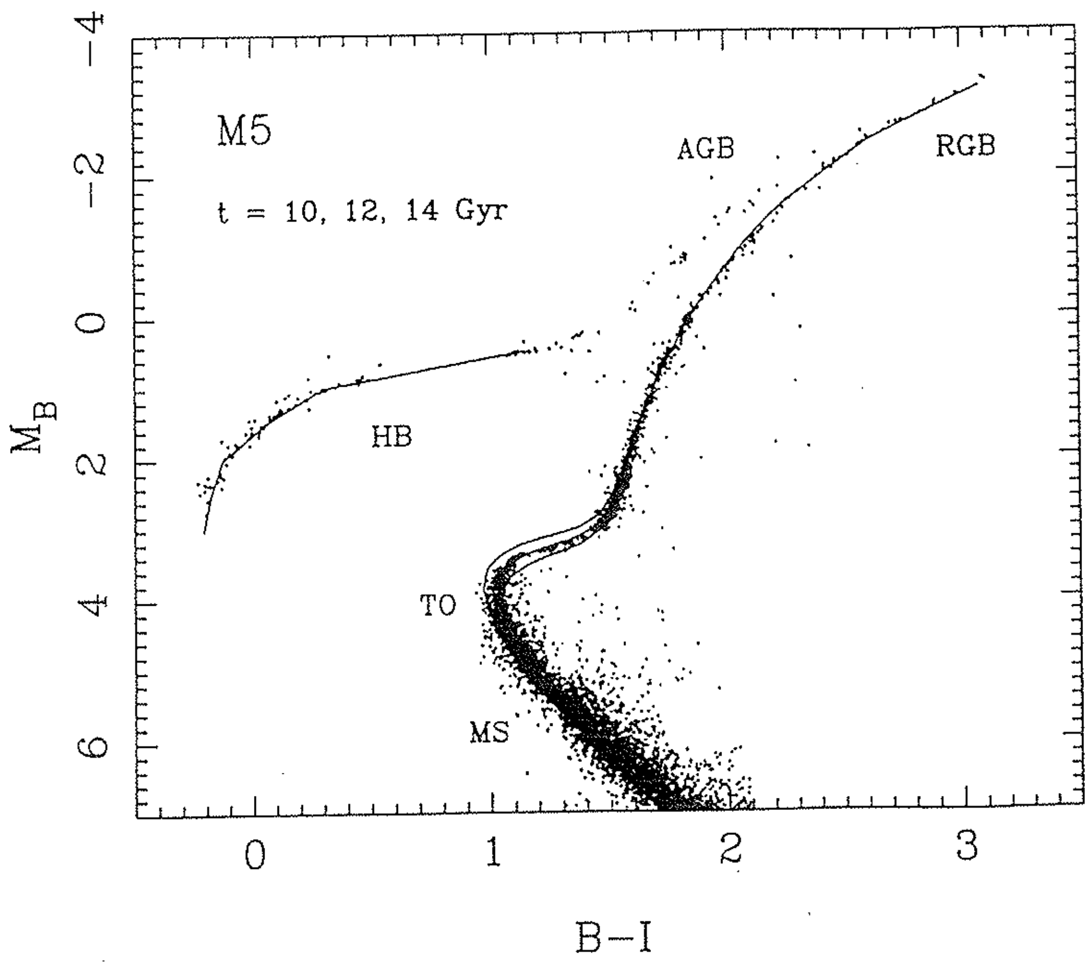

Fig 5.9

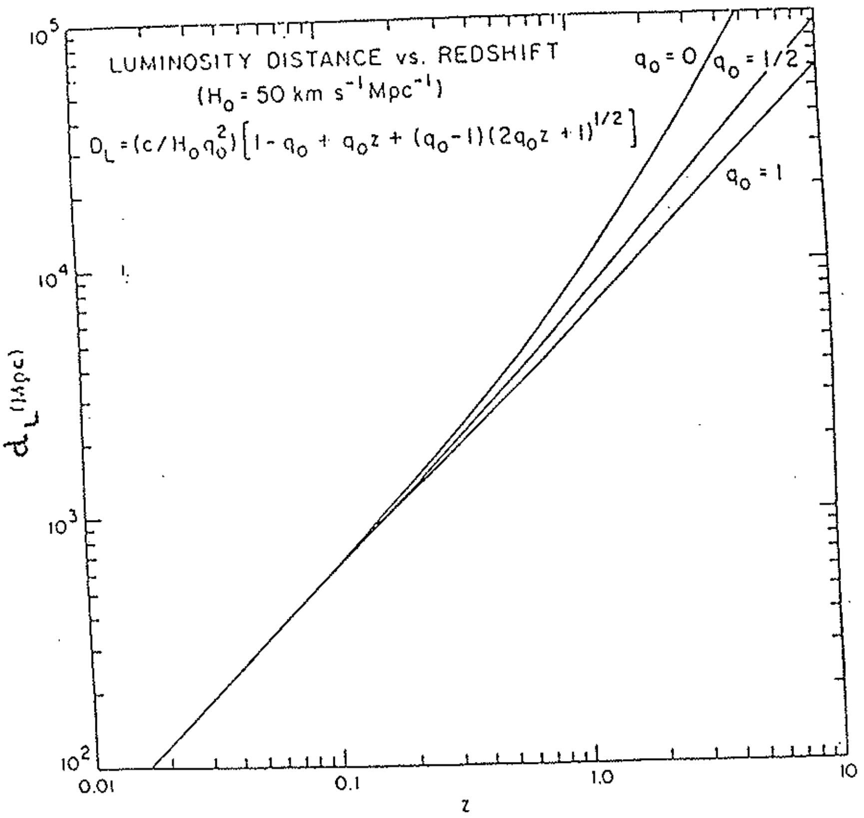

$$D_L = \frac{2c}{H_0}\,\frac{\Omega_0 z + (\Omega_0 - 2)\left[\sqrt{1+\Omega_0 z} - 1\right]}{\Omega_0^2(1+z)}$$

pressureless matter

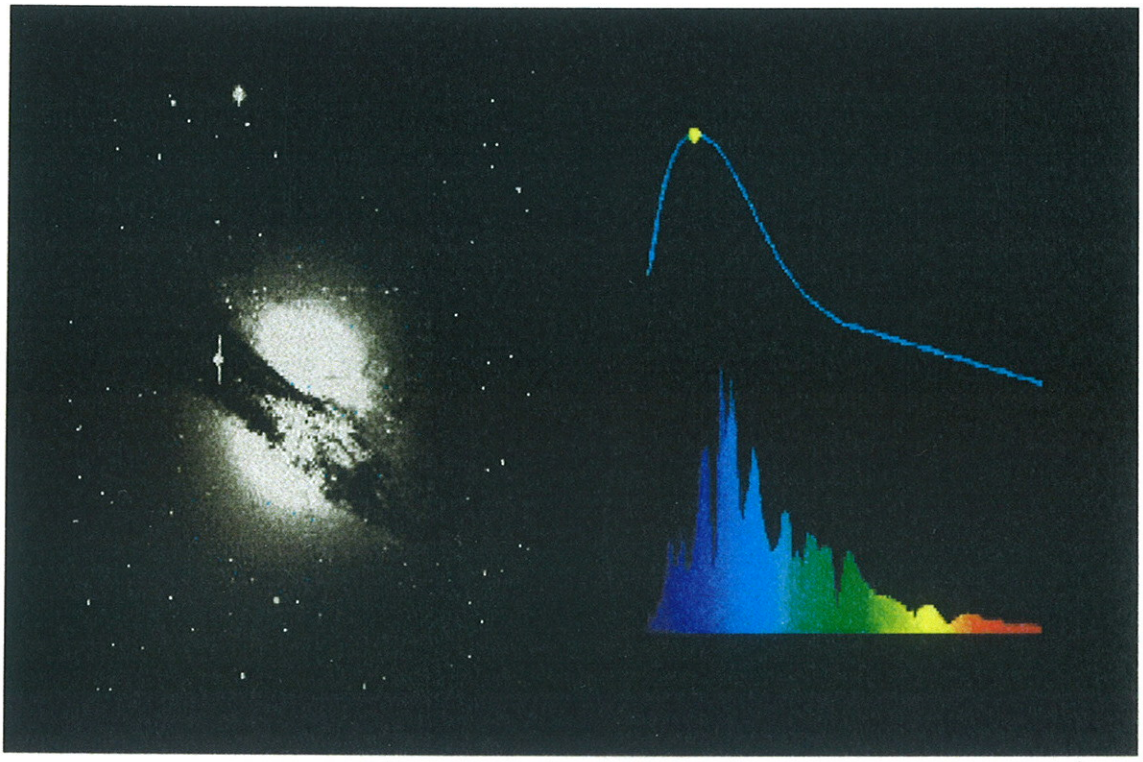

A simulation of a supernova explosion that occurred recently in the galaxy Centaurus A. The brightness of the supernova becomes comparable to that of the entire galaxy. The figure on the upper right shows how the brightness varies with time. The change of the star's spectrum with time is shown in the bottom right figure.

Fig 5.3

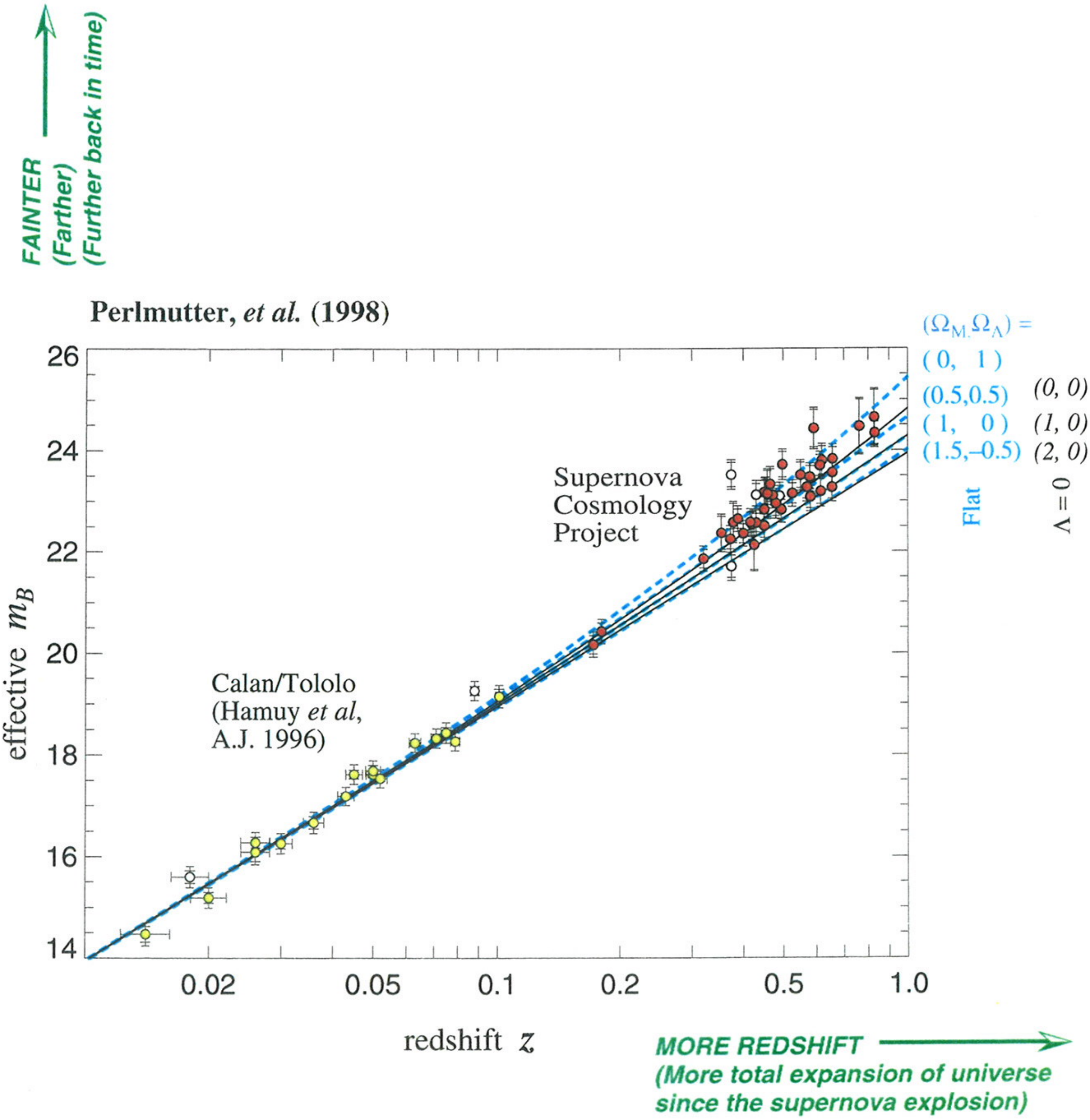

In flat universe: $\Omega_M = 0.28$ [± 0.085 statistical] [± 0.05 systematic]

Prob. of fit to $\Lambda = 0$ universe: 1%

Fig 6.4

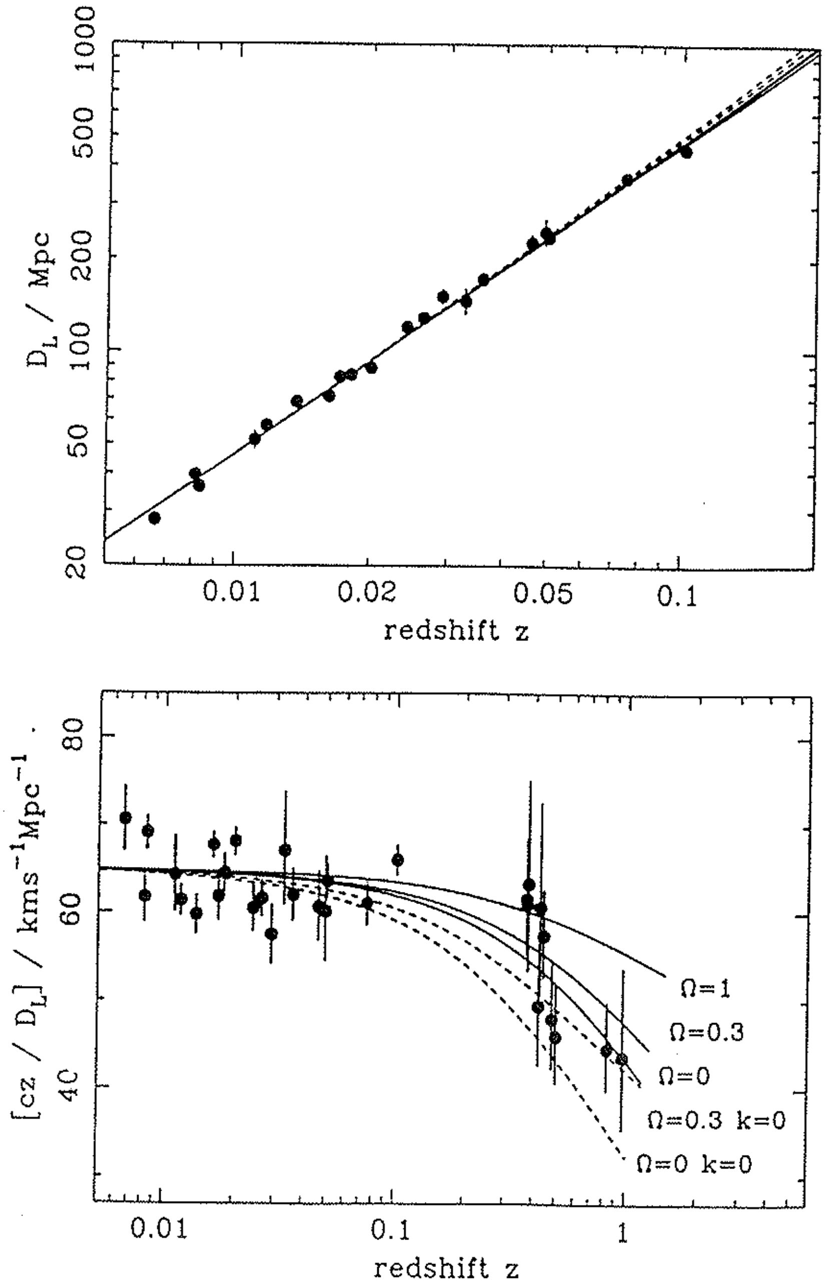

The type Ia supernovae Hubble diagram. The top figure is up to a redshift of 0.1 and shows that the Hubble flow is linear and uniform. The best-fit value for the Hubble constant is $H_0 = 64 \pm 3\,\mathrm{km\,s^{-1}\,Mpc^{-1}}$. The lower figure is for redshifts to $z \approx 1$. The ratio z/D_L is plotted, so a linear relation would correspond to a horizontal line. Deviations from linearity are seen. The three solid curves represent what should be observed if the universe contains only pressureless matter for three different values of Ω_0. The data does not fit these curves well. The two dashed curves are for models containing a cosmological constant (see later).

Fig 6.4a

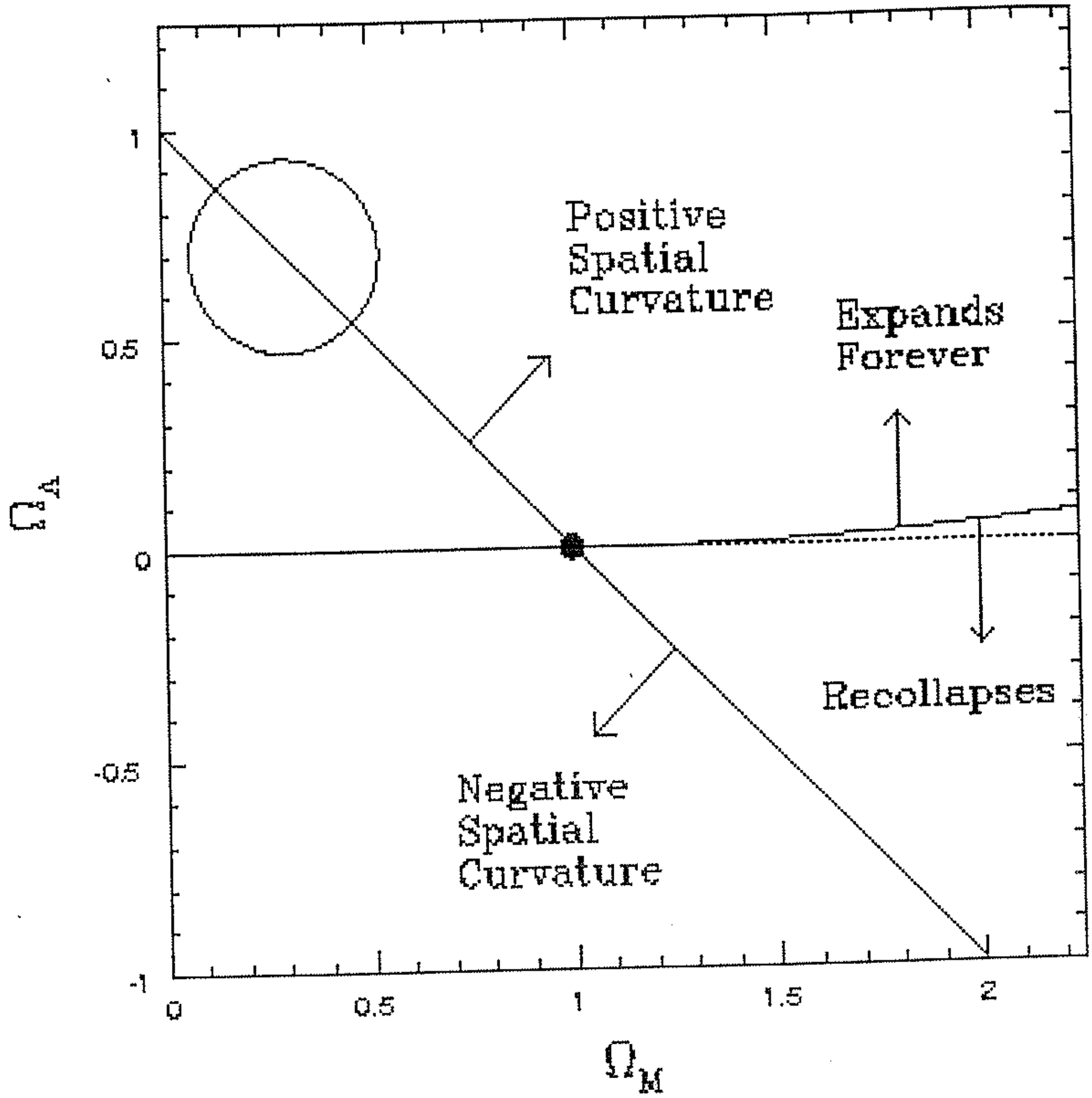

Illustrating the effect of a cosmological constant on the fate of the universe. The Ω-parameter of the cosmological constant is plotted with that of ordinary (pressureless) matter, Ω_M. The diagonal straight line correponds to a spatially flat universe, where $\Omega_\Lambda + \Omega_M = 1$. The dot in the middle corresponds to the spatially flat, pressureless universe. The circle to the top left of the figure represents the region consistent with observations from high redshift supernovae.

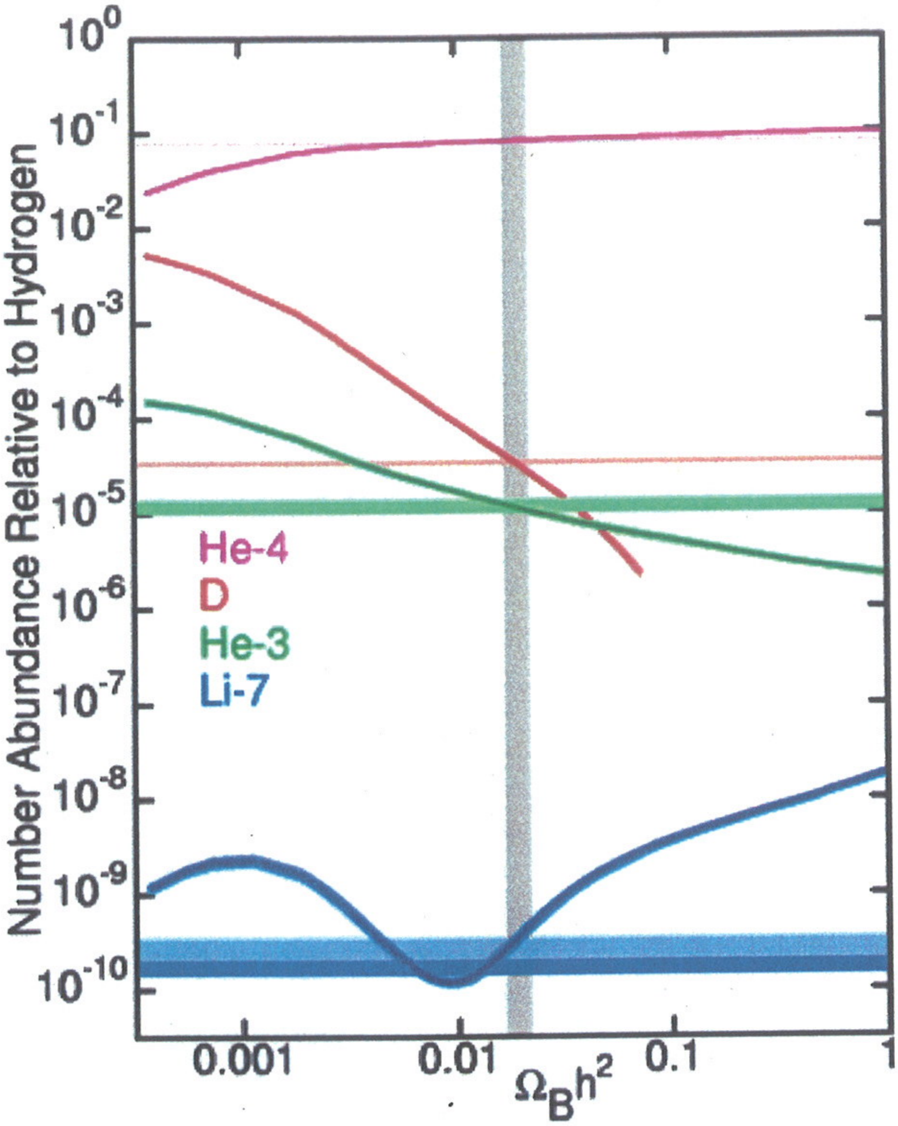

Fig. (9.1). The predicted abundances of the light elements (curves) compared with the observations (horizontal bands). The abundances depend on the baryon density. The horizontal axis denotes present–day values for the baryon density, Ω_B, measured in units of the critical density. The vertical band denotes the range of baryon densities where the data is consistent with the theoretical predictions. Remarkably, there is agreement between theory and observation for all four light element abundances if the baryon density is in the range $\Omega_B h^2 = 0.013 \pm 0.002$. It is significant that this implies that the baryon density is considerably less than the critical density.

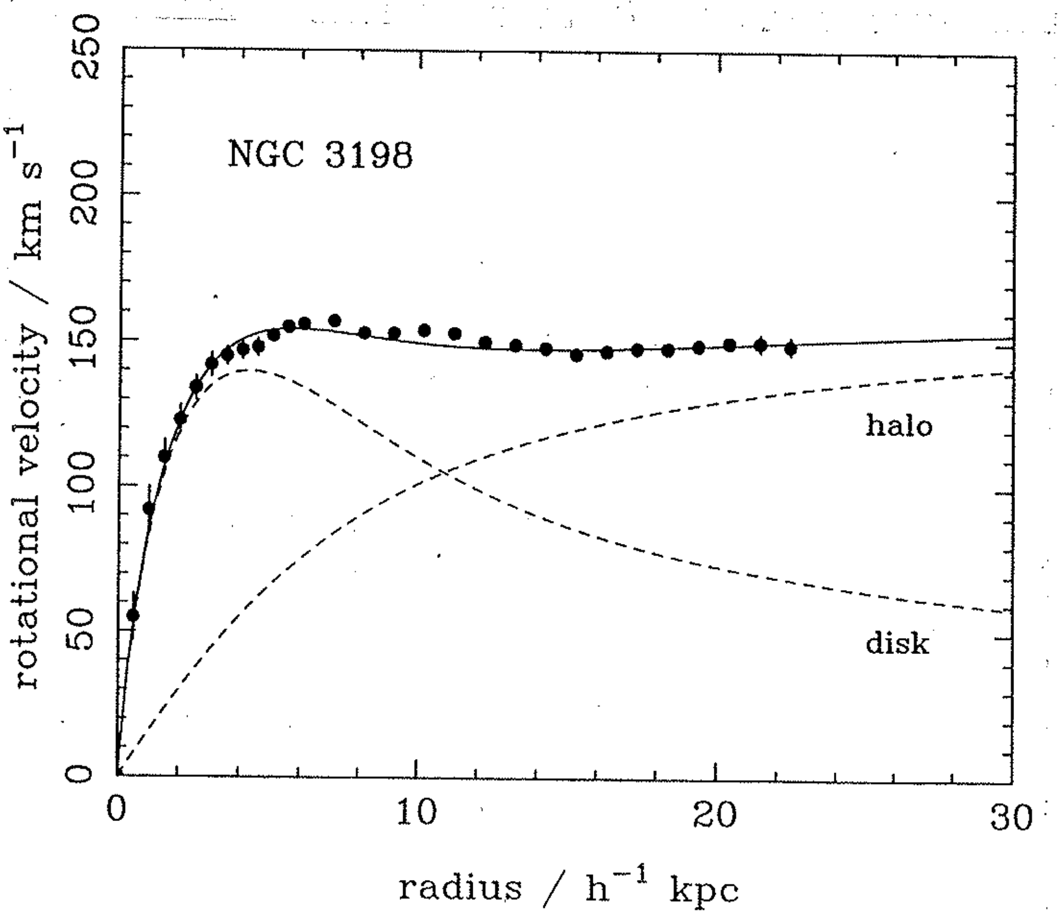

10.1

Figure ~~12.4~~. The brightness profile and rotation curve of the spiral galaxy NGC3198 (adapted from van Albada *et al.* 1985). Note the flat form of the curve at large radii by comparison with the contribution expected from the luminous disk.

Fig 10.1

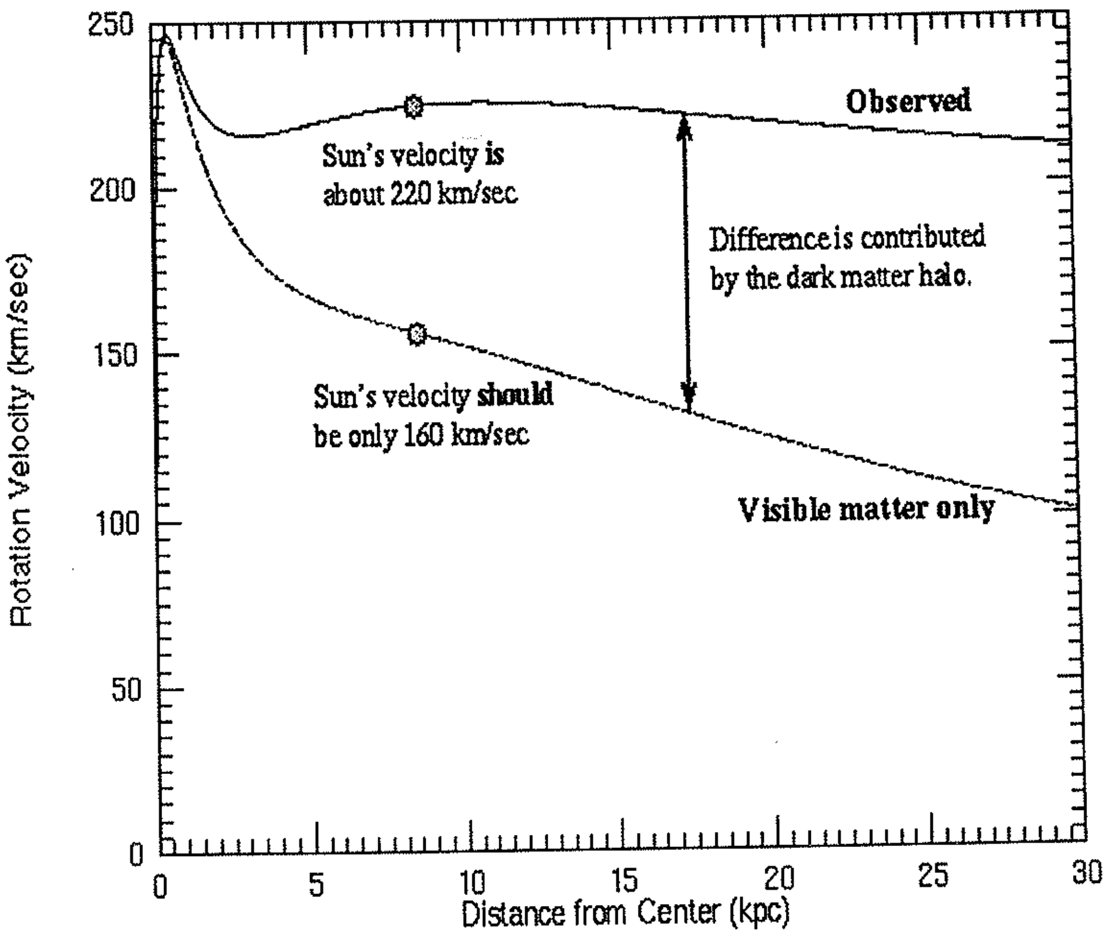

The gravity of the visible matter in the Galaxy is not enough to explain the high orbital speeds of stars in the Galaxy. For example, the Sun is moving about 60 km/sec too fast. The part of the rotation curve contributed by the visible matter only is the bottom curve. The discrepancy between the two curves is evidence for a **dark matter halo.**

Fig 10.2

Cosmic Microwave Background

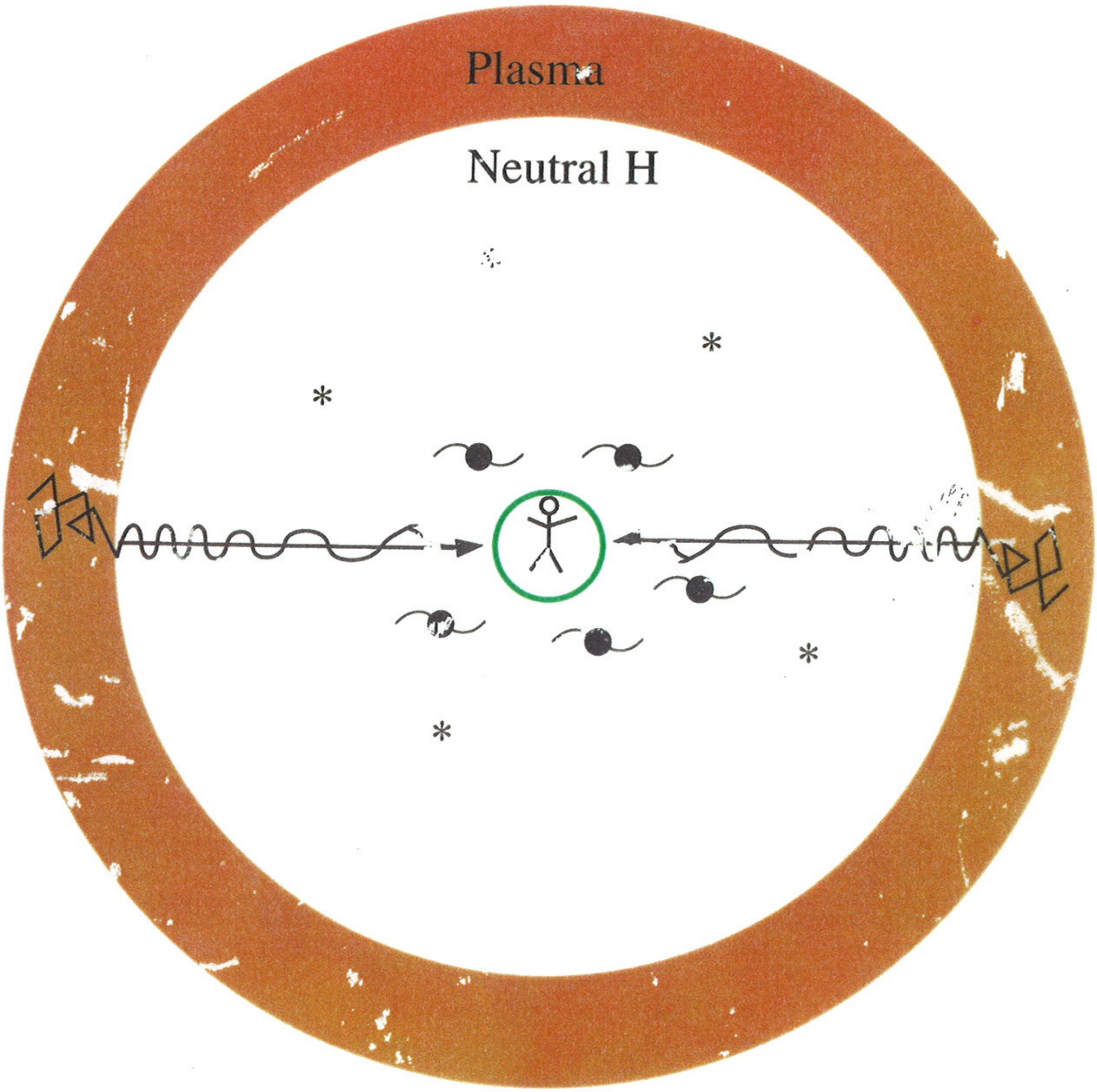

Fig 13.1

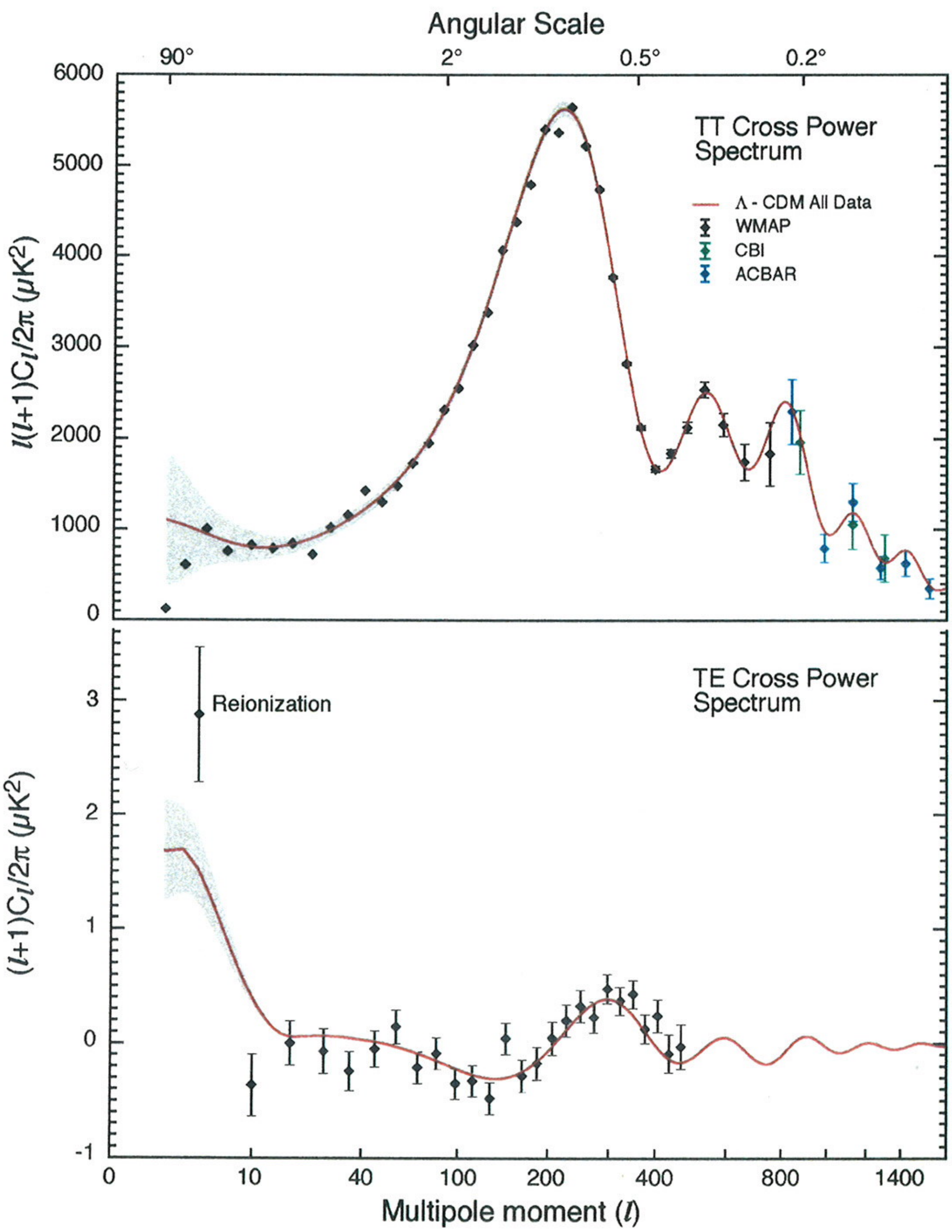
Angular Scale
90°
2°
0.5°
0.2°
6000
5000
4000
3000
2000
1000
0
TT Cross Power Spectrum
Λ - CDM All Data
WMAP
CBI
ACBAR
$l(l+1)C_l/2\pi$ (μK^2)
3
2
1
0
-1
Reionization
TE Cross Power Spectrum
$(l+1)C_l/2\pi$ (μK^2)
0
10
40
100
200
400
800
1400
Multipole moment (l)

Fig 13.2

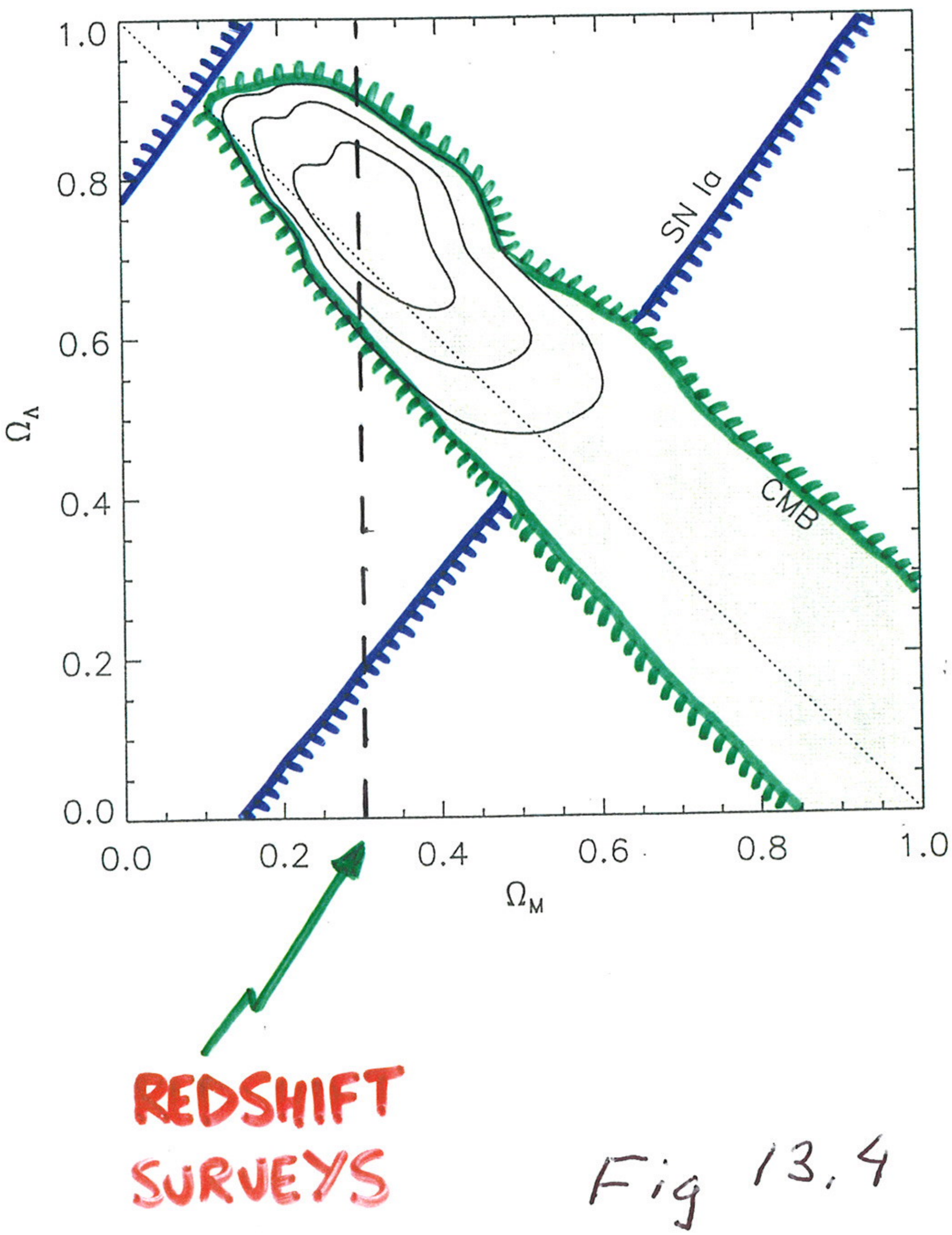

Fig 13.4

High Z- Supernova Search Team (2001)

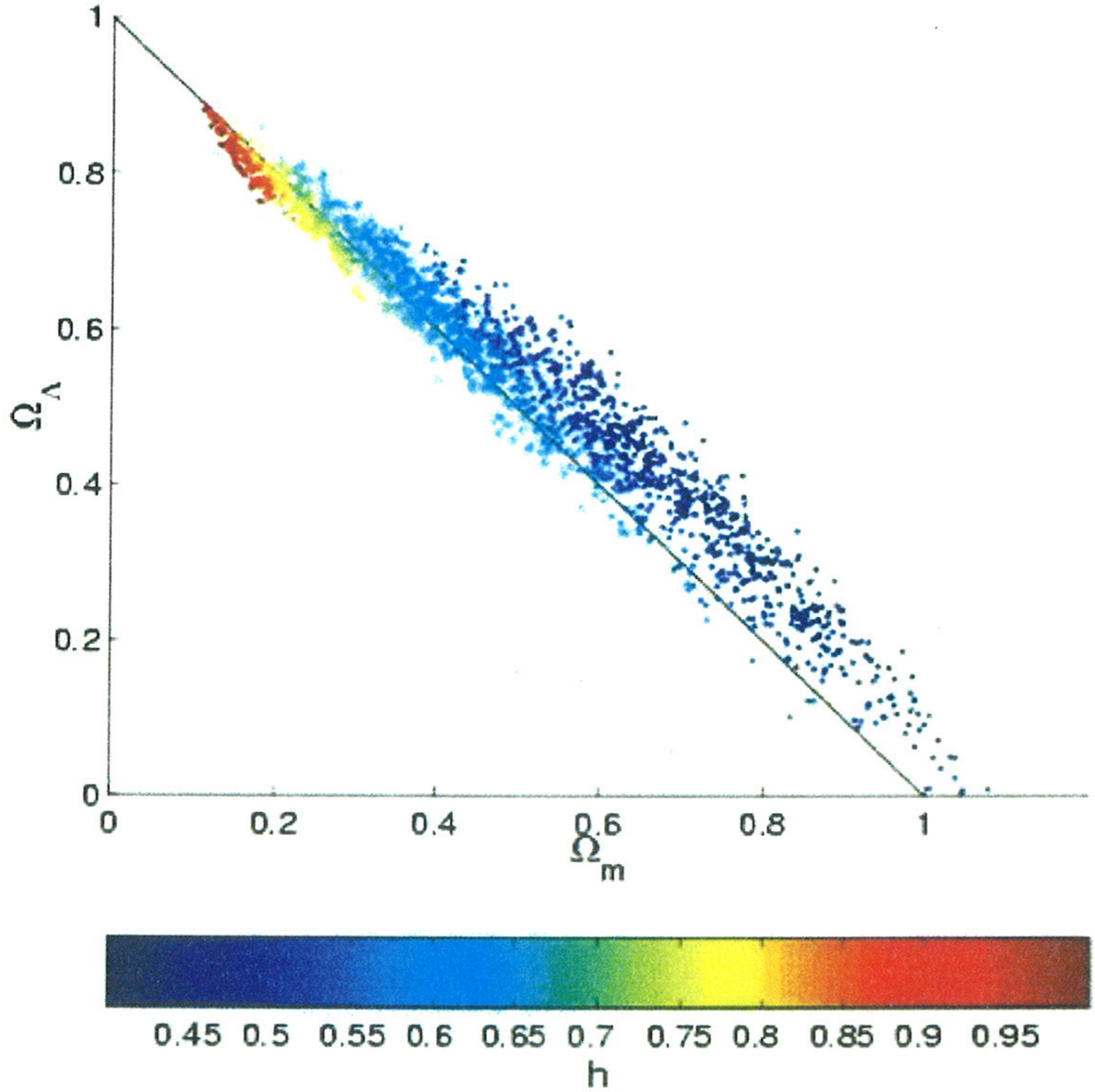

Fig. 11.3. Illustrating the favoured values for the density of the cosmological constant (Ω_Λ) and that of matter (Ω_m). The data is taken from the high redshift supernovae surveys and observations of the temperature fluctuations in the cosmic microwave background. These latter observations are sensitive to the total density of the universe and allow the value of $\Omega_{total} = \Omega_\Lambda + \Omega_m$ to be deduced. The data strongly favours a universe where the total density is close to the critical density, corresponding to the diagonal straight line. The relative densities of the cosmological constant and matter are sensitive to the value of the Hubble constant, h. For the favoured value of $h = 0.65$ (see Section 6), the best-fit to the data is for $\Omega_\Lambda = 0.7$ and $\Omega_m = 0.3$. The data is consistent with the central prediction of inflation that Ω_{total} should be very close to unity.

Fig 13.5